ELSEVIER

S0032-3861(96)00460-0

Polymer Vol. 37 No. 26 pp. 5889–5896, 1996

0032-3861/96/$15.00 + 0.00

Unimolecular-micelle formation of poly(methyl methacrylate)-*graft*-polystyrene in iso-amyl acetate

Atsushi Kikuchi and Takuhei Nose*

Department of Polymer Chemistry, Tokyo Institute of Technology, Ookayama, Meguro-ku, Tokyo 152, Japan

(Received 29 February 1996; revised 25 March 1996)

By means of light scattering, unimolecular-micelle formation is investigated for poly(methyl methacrylate)-*graft*-poly(styrene)s with different graft-chain densities in a dilute solution of a selective solvent. Molecular weights of the poly(methyl methacrylate) (PMMA) backbone and the branch poly(styrene) (PS) are about 6×10^6 and 9×10^3, respectively, and the graft-chain density is relatively low, ranging from 6 to 17 of PS composition in wt%. The solvent used is iso-amyl acetate, which is a thermodynamically good solvent for PS and a poor solvent (θ-temperature: 60°C) for PMMA. Radius of gyration, hydrodynamic radius, and the second virial coefficient are measured as a function of temperature ranging from 10 to 70°C. At a branch PS composition of 6 wt%, with decreasing temperature, the copolymer chain shrinks in the same manner as the PMMA chain with no PS branches, although the θ-temperature decreases by about 25°C. This indicates that no particular order structure is formed. At higher branch densities, rod-like unimicelles are strongly suggested to be formed by intramolecular segregation between the PMMA backbone and PS branches, with the shrunken PMMA backbone forming the core rod covered with PS chains. With decreasing temperature, the dimension of the unimolecular micelle decreases probably due to decreasing contour length of the micelle core. Copyright © 1996 Elsevier Science Ltd.

(Keywords: graft copolymer; characterization; unimolecular micelle)

INTRODUCTION

Micelle formation of polymer chains in solutions of selective solvents have been studied extensively from the theoretical and experimental points of view[1–18]. Diblock and triblock copolymers form rather simple associated micelles similar to low-molecular-weight surfactants in aqueous solution. On the contrary, multi-block copolymers including graft copolymers may form a variety of micellar structures depending upon sequence and length of block chains and solvent quality by either intra- or intermolecular association. In particular, the capability of unimolecular micelle formation of the multi-block copolymers with the intramolecular association is a unique property that cannot be seen in low molecular weight surfactants, but is very common in biological macromolecules, although the structure formed is usually not a simple micelle but a more complex globule structure. For its importance, very few studies on unimolecular micelles and the association structure of multi-block copolymers or graft copolymers have been reported[19–38].

Most experimental studies on unimolecular micelles have been reported for graft copolymers. Selb and Gallot[19–24] have demonstrated that poly(styrene)-*graft*-poly(4-vinyl-*N*-ethylpyridium bromide) forms unimolecular micelles in methanol/water mixtures containing hydrogenated lithum, with the structure changing from comb-like to star-like as the water content increases. Price and Woods[25,26] have reportedly observed formation of unimolecular micelles for poly(styrene)-*graft*-poly(isoprene) in methylcyclohexane and other graft copolymers in selective solvents. Benoit *et al.* have also observed formation of unimolecular micelles for poly-(methyl methacrylate)-*graft*-poly(styrene), poly(3,3-diphenylpropene-1)-*graft*-poly(styrene) and poly(3,3-diphenylpropene-1)-*graft*-poly(methyl methacrylate) in mixed solvent of methylcyclohexane and 1,4-dioxane[27–29]. In any of the above studies, the solvents are good for branched chains, the grafted chains are rather long, for instance, one fifth of the backbone chain in the polymerization index, and the composition of the branch is larger than 50 wt%. Breslar *et al.* have reported unimolecular micelle formation of a multi-block copolymer consisting of about nine blocks of poly(styrene) and poly(isoprene)[30]. Diblock copolymers have also been reported to form unimolecular micelles[1,31–34].

As for theoretical studies, Halperin predicts that a copolymer of multi-blocks connecting alternatively form a flower-like or string of flowers unimolecular micelle in selective solvent[35]. de Gennes also predicts unimolecular micelle formation of the flower type for a statistical copolymer[36]. Joanny[37] and Khokholov[38] predict unimolecular micelle formation for a polyelectrolyte.

* To whom correspondence should be addressed

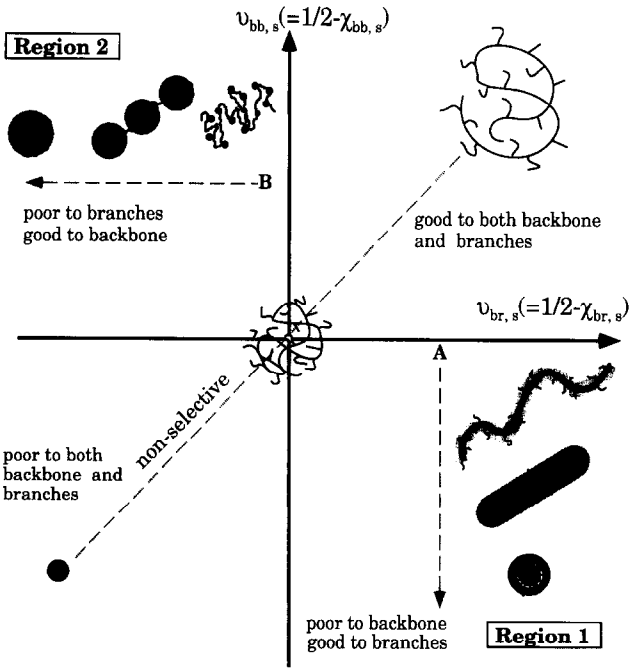

Figure 1 Schematic presentation of possible micellar structures of the graft copolymer with short branches of a low branch density as a function of solvent quality. See text for details

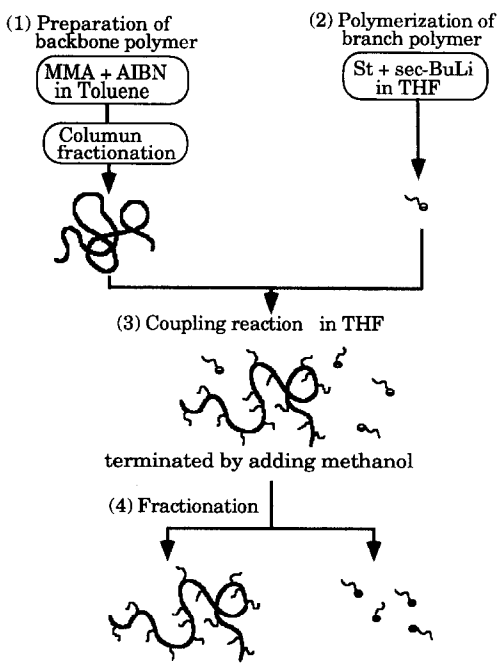

Figure 2 Scheme for preparation of PMMA-*g*-PS by coupling reaction

Micellization by intermolecular association of graft copolymers have not been so extensively studied. Dondos *et al.*[28,29], and Price and Woods[25,26] have reported associations of graft-copolymers, but not presented detailed discussion on the structure of associates.

In this series of studies, we focus our attention on unimolecular micelles and intermolecular associates formed from graft-copolymers with *low* grafted-chain densities in selective solvents.

In *Figure 1*, the predicted structures of unimolecular micelles possibly formed by such a graft copolymer are presented schematically as a function of solvent qualities to backbone chain and branch chains which are represented by excluded volume parameters $\nu_{bb,s} = 1/2 - \chi_{bb,s}$ and $\nu_{br,s} = 1/2 - \chi_{br,s}$, respectively, where χ is the monomer–monomer interaction parameter. Change of non-selective solvent quality is presented by the line $\nu_{bb,s} = \nu_{br,s}$, where the coil–globule transition observed in ordinary linear polymers will occur. If solvent quality to backbone polymer changes from nearly Θ-condition ($\nu_{bb,s} \cong 0$) to non-solvent quality ($\nu_{bb,s} \ll 0$) keeping solvent quality to branch chains good, unimolecular worm-like chain or rod micelle, where the backbone is covered with branch chains, will appear, followed by cylindrical and spherical unimolecular micelles as shown along the line A in region 1. In contrast, in region 2, as the solvent quality of branches becomes poorer from nearly Θ-condition ($\nu_{br,s} \cong 0$) at a fixed $\nu_{bb,s}$ (> 0) solvent, as illustrated by line B, a unimolecular micelle of flower-connecting type will be formed via petals of random coil structure with a centre core of shrunken branch chains. In the non-solvent quality limit ($\nu_{br,s} \ll 0$), a unimolecular micelle made up of one flower will be formed. Detailed structures of unimolecular micelles, such as petal number per flower, may depend on branch density and length ratio of branch chain to backbone chain as well as solvent quality including selectivity.

In addition to the case of unimolecular micelles, in the formation of multimolecular micelles, a variety of structures can be supposed depending on the method of intermolecular association.

To reveal the predicted behaviour mentioned above and other behaviours of graft-copolymer with *low* grafted-chain densities in selective solvents, we require systematic experimental studies. For this purpose, we synthesized neat samples of poly(methyl methacrylate)-*graft*-poly(styrene) (PMMA-*g*-PS) consisting of a long backbone and short branches, where the branches are 1/600 shorter in molecular weight than the backbone, having different branch densities in the range of 6–17 wt% of branched chains in a copolymer chain.

In this study, we investigate unimolecular micelles of PMMA-*g*-PS formed in iso-amyl acetate (i-AA) which is a thermodynamically good solvent to branched PS and a theta (θ) solvent to the PMMA backbone to reveal micelle-forming conditions and the structure as a function of solvent quality (i.e. temperature) and branch density. That is, we study the unimolecular micelle formation in region 1 shown in *Figure 1*.

In the following section, we will first describe details of PMMA-*g*-PS sample preparation, and then method and analysis of light-scattering experiments, and present the experimental results of molecular weight, radius of gyration, hydrodynamic radius, and the second virial coefficient, followed by estimated unimolecular micelle structures.

EXPERIMENTAL

Materials

Graft copolymers used were newly synthesized (CL-1, CL-2) and one (RS-8) previously made using macromonomers[39].

Table 1 Characteristics of PMMA-*g*-PS samples (CL-1, CL-2 and RS-8)

Sample	Backbone (CL-b)		Branch		
	M_w^a (10^6 g mol^{-1})	M_w/M_n^b	M_w^b (10^3 g mol^{-1})	M_w/M_n^b	Average PS composition[c] ($\langle w \rangle$)
CL-1	5.58 (6.02[b])	<1.10	8.77	1.07	0.0614
CL-2	5.58 (6.02[b])	<1.10	9.19	1.04	0.128
RS-8	5.96	—	8.52	1.10	0.175

[a] Measured by SLS
[b] Measured by s.e.c.
[c] Measured by ^{1}H n.m.r.

Preparation of graft copolymers CL-1 and CL-2

Poly(methyl methacrylate)-*graft*-polystyrene (PMMA-*g*-PS) was prepared by the processes with coupling reaction as illustrated schematically in *Figure 2*. In process (1), poly(methyl methacrylate) (PMMA) was made by radical polymerization using azobisisobutyronitrile (AIBN) as initiator in toluene, followed by molecular weight fractionation by a preparative size exclusion chromatography. The PMMA sample obtained was named CL-b and used as the backbone chain. Living polystyrene (PS) to be grafted to chains was anionically polymerized in tetrahydrofuran (THF) with *sec*-butyl lithium as initiator [process (2)]. The fractionated PMMA and living PS were reacted in THF at −78°C to form graft copolymers, PMMA-*g*-PS, and the living ends of the unreacted PS were killed by adding a small amount of methanol [process (3)]. The coupling reaction was performed for two different PMMA/PS compositions to obtain PMMA-*g*-PS with different branch densities. The product of coupling reaction was purified by removing unreacted PMMA and PS by means of extraction using acetonitrile and cyclohexane and repeated precipitations by toluene/cyclohexane solvent systems [process (4)].

Pre-treatment and stability

As-synthesized PMMA-*g*-PS in solutions of THF and some other solvents showed molecular weights 2–3 times larger than the expected one, and a broad molecular weight distribution, suggesting intermolecular associations due to insufficient dissolution. This problem was not solved by using other solvents, leaving for a long time with stirring, and/or heating up to about 60°C, but disappeared using methyl ethyl ketone and ethyl acetate. Once the sample was dissolved molecularly, then no such 'association' was observed even in a solution of other solvents. In view of this fact, the as-synthesized graft copolymers were first dissolved in ethyl acetate, followed by complete evaporation of the solvent, and dried by the freeze-dry method with benzene.

The graft copolymer was stable, showing no degradation in solution for more than 10 days around 60°C. All the experiments were performed watching the sample stability.

Characterization

Weight-average molecular weight M_w and polydispersity index M_w/M_n of PMMA backbones and PS branches for two PMMA-*g*-PS (sample codes CL-1 and CL2) used in this study were determined by light scattering and analytical size exclusion chromatography (s.e.c.). Chemical composition was determined from ^{1}H n.m.r. spectra in deuterated methylene dichloride measured by a 500 MHz n.m.r. spectrometer, JEOL GSX 500 (*Table 1*). CL-1 and CL-2 consist of the same backbone-chain length and almost the same branch length with narrow molecular-weight distributions, but have different branch densities.

Molecular weight distribution (MWD) and chemical composition distribution (CCD) of PMMA-*g*-PS were characterized by light scattering using three solvents: 1-ethyl naphthalene (1-EN), chloroform (CHF), and i-amyl acetate (i-AA) with different refractive indices n ($n = 1.61$, 1.44, and 1.35, respectively, while $n = 1.5$ and 1.6 for PMMA and PS, respectively). The three solvents gave the same apparent molecular weight within experimental error, as shown in *Figure 3*, consistent with the one calculated from molecular weights of backbone PMMA and branch PS and average chemical compositions. This implies that both MWD and CCD are reasonably narrow[39,40]. That is, the apparent molecular weight M_w(apparent) observed by light scattering does not give the true M_w in the case of the copolymer, but depends on the refractive index of solvent following the relation[40]

$$M_w(\text{apparent}) = M_w(\text{true})(1 + 2\tilde{P}b + \tilde{Q}b^2) \quad (1)$$

Here, b is given by $b = (\nu_A - \nu_B)/\nu_0$, where ν_A, ν_B and ν_0 are the refractive index increment of the polymers forming the two types of block and the copolymer mixture, respectively. The two parameters $\tilde{P}$ and $\tilde{Q}$ are related to the heterogeneity of composition of the sample. The results of *Figure 3* show that $\tilde{P}$ and $\tilde{Q}$ almost vanish, indicating very narrow MWD and CCD.

The narrow molecular weight distribution was also confirmed by s.e.c. measurements, which gave $M_w/M_n = 1.08$ for CL-1 and 1.15 for CL-2.

Characteristics of RS-8 prepared in the previous study[39] are listed in *Table 1*. The branch density is higher than those of CL-1 and CL-2. For the three graft copolymers, backbone length and branch length are

Table 2 Average number, m, of branches and average molecular weight, M_{sc}, between nearest neighbour branching points

Sample	m^a	M_{sc}^b (10^4 g mol^{-1})
CL-1	42.6	13.4
CL-2	93.2	6.26
RS-8	137	4.03

[a] Calculated from $M_w\langle W \rangle/M_w$ (branch). M_w of CL-1, CL-2 and RS-8 are 6.09×10^6, 6.69×10^6 and 7.22×10^6 g mol^{-1}, respectively
[b] Calculated from $M_w(1 - \langle W \rangle)/m$

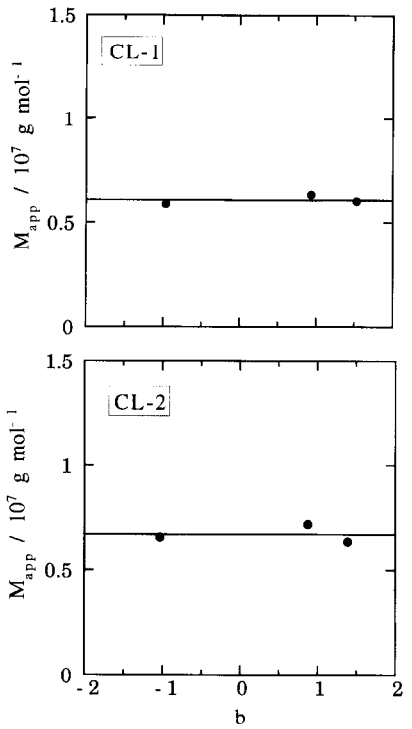

Figure 3 Plots of apparent molecular weight, M_{app}, vs b for CL-1 and CL-2. Solvents are 1-EN, i-AA, CHF from left to right. $b = (\nu_{PS} - \nu_{PMMA})/\nu_0$, where ν_{PS}, ν_{PMMA} and ν_0 are refractive-index increments of PS, PMMA, and copolymer, respectively. The solid line is the average value of M_{app} in the three solvents

almost the same. It should be noted that the MWD and CCD of RS-8 are not as narrow as those of CL-1 and CL-2. The true M_w listed in *Table 1* was evaluated using equation (1), where $\tilde{P}$ and $\tilde{Q}$ were 0.44 and 0.51, respectively. In *Table 2* are listed values of average numbers, m, of branches and average molecular weight, M_{sc}, between nearest neighbour branching points for graft copolymers. The branch number m ranges from 40 to 140, and the molecular weights, M_{sc}, are 4–14 times larger than the molecular weight of branches indicating a low grafted-chain density.

Light scattering measurements

Light scattering measurements were carried out in iso-amyl acetate (i-AA). Purchased i-AA was dried over calcium hydride, and purified by distillation. Sample solutions were filtered through a Millipore filter into light scattering cells, followed by dilution with dust-free solvent to the desired concentration. The optical cells were subsequently flame-sealed under vacuum.

The light scattering apparatus was specially designed with Ar-ion lasers of wavelength 488 nm as light source, using the photon-counting method. Details of the light scattering spectrometer have been described elsewhere[41]. The excess Rayleigh ratio $[R_{vv}(\theta)]$ for vertically polarized incident and scattered light was extrapolated to zero concentration (C) and zero angle (θ) by Zimm plots or Berry plots to determine molecular weight M_w, radius of gyration R_g, and the second virial coefficient A_2, following the equation

$$\frac{KC}{R_{vv}(\theta)} = \frac{1}{M_w}\left[1 + \frac{R_g^2}{3}q^2 + \cdots\right] + 2A_2C + \cdots \quad (2)$$

where the constant K is given by $K = 4\pi^2 n^2 (\partial n/\partial C)^2/(N_A\lambda_0^4)$, with n being the refractive index of solvent, N_A the Avogadro constant, $(\partial n/\partial C)$ the refractive index increment, and λ_0 the wavelength of the incident beam in vacuum, and the momentum transfer q is given by $q = (4\pi n/\lambda_0)\sin(\theta/2)$. The concentration C is in weight per volume of solution. The value of R_g is the refractive-index-increment weighted in copolymers. In the present case, however, the scattered light intensity of the PMMA backbone dominates over that of PS branches because of the low branch composition, so that the obtained R_g can be practically regarded as a true radius of gyration of z-average (estimated discrepancy was about 5% in the case of core-corona sphere micelle).

The values of R_g and A_2, as well as M_w, thus obtained are apparent depending on the refractive indices of solvents for a copolymer solution with polydispersity in chemical composition. Although this is the case for the copolymer RS-8, the apparent values of R_g and A_2 were used without any correction because the polydispersity was not so large. The apparent values may reflect the components with larger PS compositions having the larger refractive index increment. In this sense, the meaning of the values of R_g and A_2 is not so clear for RS-8 as for the other samples.

Since, in the measurements of CL-b solution at low temperature ($\leq$40°C), the extrapolation to the dilute limit was not available because of aggregation, we evaluated apparent values of M_w and R_g without the extrapolation, which are defined as

$$M_w = \frac{R_{vv}(0)}{KC} \quad (3)$$

$$R_g^2 = \frac{M_w(\text{initial slope})}{q^2/3} \quad (4)$$

where $KC/R_{vv}(0)$ and (initial slope) are the intercept and the initial slope of $KC/R_{vv}(\theta)$ vs q^2 plot at finite concentration. Since the polymer concentration was low [2.55×10^{-4} g (g of solution)$^{-1}$], the apparent values were treated as true ones.

The refractive indices and densities of the solvents were obtained by extrapolation of the reported values to the desired wavelength and temperature[42,43]. For the refractive index increment of PS, PMMA, and the graft copolymers, reported values[44] and measured values using a differential refractometer (Union Giken RM-102) were used.

The correlator used for dynamic light scattering was a multiple tau digital correlator ALV-5000. The correlation function of electric field obtained from the autocorrelation function of scattered light intensity approximately followed a single exponential decay and allowed us to obtain the decay rate Γ by the second order cumulant method[45]. The Γ-value showed a q-square dependence as all the experimental conditions satisfied $R_g q < 1$. The diffusion coefficient D was evaluated by $D = \Gamma/q^2$, and extrapolated to zero concentration to obtain the diffusion coefficient D_0 at the infinitely dilute limit. The obtained D_0 was transformed to the hydrodynamic radius R_h by the Einstein–Stokes equation

$$R_h = \frac{kT}{6\pi\eta D_0} \quad (5)$$

Table 3 R_g and A_2 of CL-b, CL-1, and CL-2 in non-selective good solvents, chloroform (CHF) and 1-ethyl naphtharene (1-EN)

	R_g (nm)		A_2 (10^{-5} cm^3 mol g^{-2})	
Sample	1-EN	CHF	1-EN	CHF
CL-b	115	—	20.7	—
CL-1	124	135	18.9	21.3
CL-2	134	121	16.4	20.7

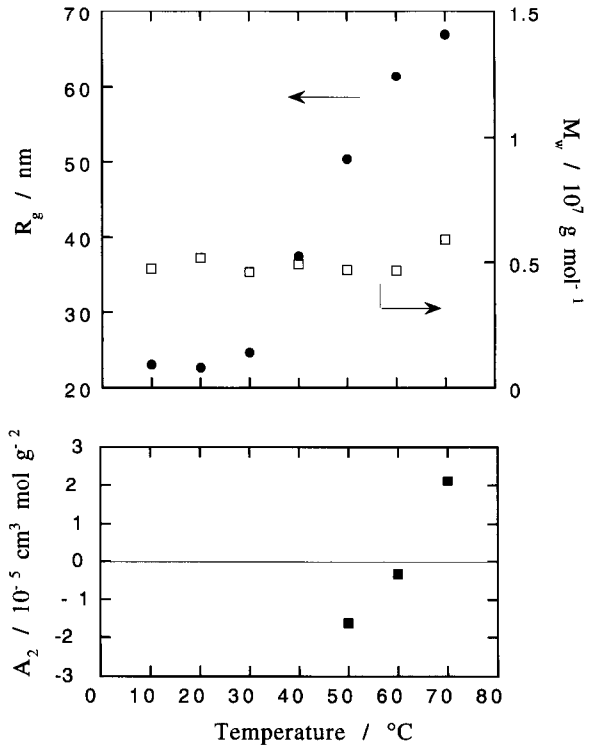

Figure 4 Changes of M_w (□), R_g (●) and A_2 (■) of Cl-b in i-AA with decreasing temperature

where k, T and η are the Boltzman constant, absolute temperature and solvent viscosity. The viscosity η was measured by an Ubbelohde-type viscometer as a function of temperature.

In the measurements of Cl-b solution at low temperatures, the apparent R_h was evaluated using the diffusion coefficient D at finite concentration directly to the Einstein–Stokes equation. The apparent values were regarded as true ones.

RESULTS AND DISCUSSION

R_g and A_2 in non-selective good solvents

Values of R_g and A_2 for CL-1, CL-2, and PMMA backbone, CL-b, in *non*-selective good solvents, 1-ethyl naphthalene (1-EN) and chloroform (CHF) are listed in *Table 3*. As expected from low branch densities and short branches of the copolymers, changes in R_g and A_2 with grafting of branched chains are not so large.

Solvent quality of i-AA to the PMMA backbone

Figure 4 presents R_g and A_2 of CL-b in the selective solvent, i-AA, along with M_w, as a function of

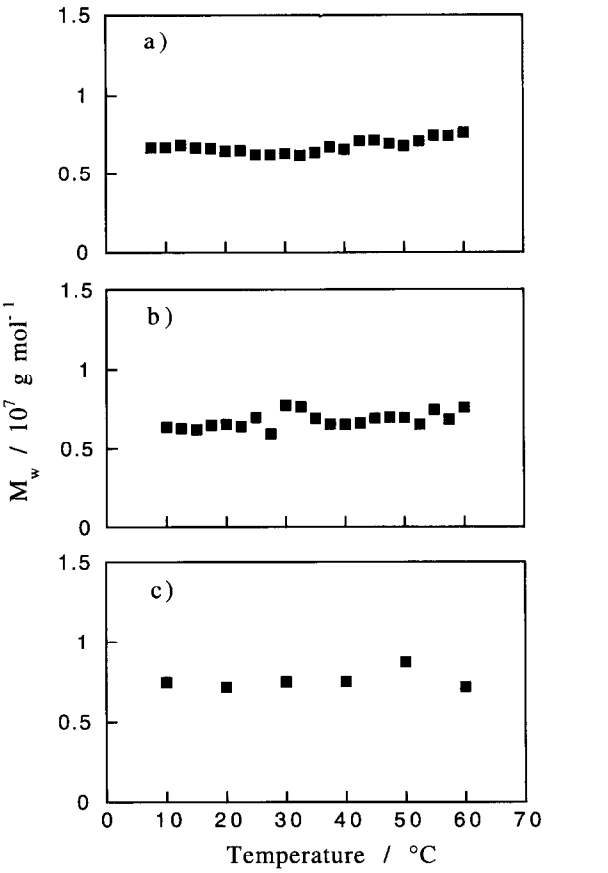

Figure 5 Change of M_w for the graft copolymers in i-AA with decreasing temperature. (a) CL-1; (b) CL-2; (c) RS-8

temperature. The θ temperature is located around 60°C, which is consistent with a reported result[44]. The chain dimension is much smaller than that in a good solvent around the θ temperature, and decreases rapidly with decreasing temperature to be that of the collapsed state. The constancy of M_w implies that, during this change, no detectable intermolecular association takes place.

R_g, R_h and A_2 of graft copolymers as a function of temperature and branch density

Figure 5 presents the temperature dependence of M_w for the copolymers CL-1, CL-2 and RS-8 in the selective solvent, i-AA, which shows that no appreciable association took place in any of the graft copolymers.

R_g's of CL-1, CL-2, RS-8, and CL-b in i-AA as a function of temperature are shown in *Figure 6*. R_g's of the graft copolymers are larger than that of CL-b with no PS branches, as expected, because the presence of PS branches, which have repulsive interaction in i-AA, i.e. positive excluded volume, may expand the chain dimension whatever the chain-conformational structure is. At higher temperatures around 60°C, R_g of Cl-1 with the lowest branch density is the largest and R_g seems to decrease with increasing branch density (BD) in the present range of BD. The temperature dependence of R_g of Cl-1 is very similar to that of CL-b, while those of CL-2 and RS-8 are weaker than that of CL-b and the dependence becomes weaker as BD increases. This means that the higher BD is larger at lower temperature.

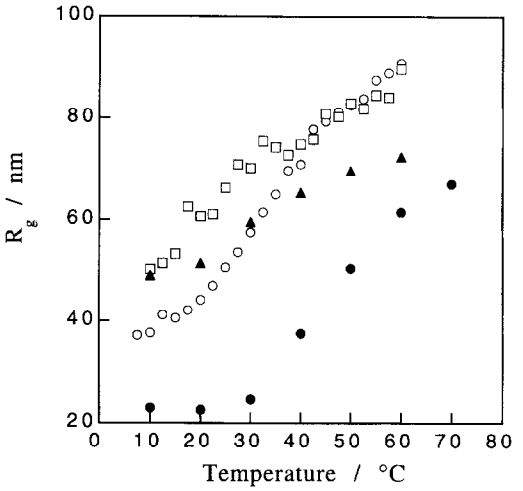

Figure 6 Change of R_g with decreasing temperature for the graft copolymers and the backbone polymer in i-AA. (○) CL-1; (□) CL-2; (▲) RS-8; (●) CL-b

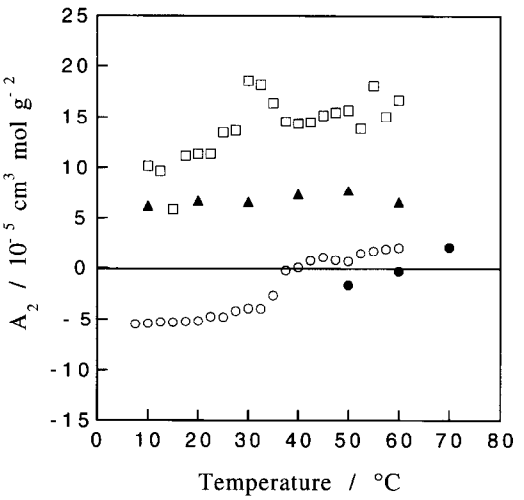

Figure 7 Change of A_2 with decreasing temperature for the graft copolymers and the backbone polymer in i-AA. (○) CL-1; (□) CL-2; (▲) RS-8; (●) CL-b

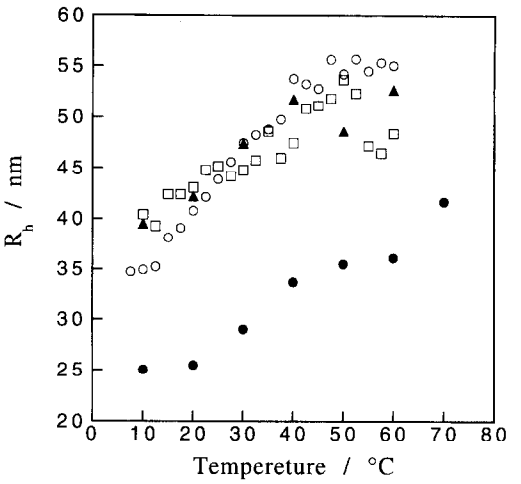

Figure 8 Change of R_h with decreasing temperature for the graft copolymers and the backbone polymer in i-AA. (○) CL-1; (□) CL-2; (▲) RS-8; (●) CL-b

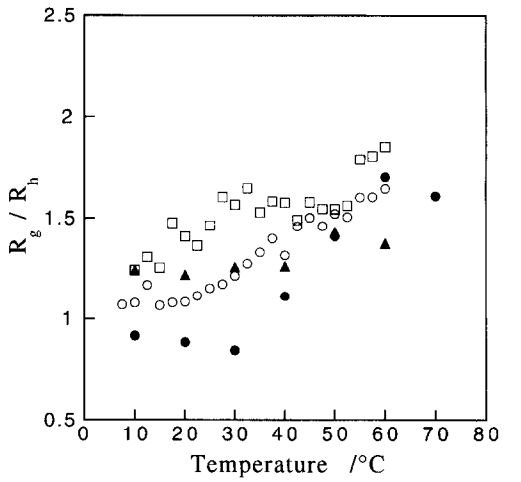

Figure 9 Change of R_g/R_h with decreasing temperature for the graft copolymers and the backbone polymer in i-AA. (○) CL-1; (□) CL-2; (▲) RS-8; (●) CL-b

It is noteworthy that the R_g-behaviour does not seem to change monotonously with increasing BD, but those of CL-2 and RS-8 are different from that of CL-1.

This characteristic for the changes in R_g-behaviour with BD is more clearly seen in the behaviour of the second virial coefficient A_2, which is shown in *Figure 7*, where A_2 is plotted against temperature T. The most characteristic feature is the difference between CL-1 and CL-2 or RS-8. Namely, the magnitude and temperature-change of A_2 in CL-1 are similar to that of CL-b, although the A_2-T plots shift to lower temperatures from those for CL-b, having a θ temperature around 35°C, whereas A_2 of CL-2 and RS-8 have larger positive values in the whole temperature range. Compared with CL-2, the copolymer RS-8 exhibits smaller A_2 values at higher temperatures, and a weaker temperature dependence to have similar values of A_2 at lower temperatures.

Figure 8 shows the R_h results. The hydrodynamic radii of the graft-copolymers are much larger than that of the backbone, and have very weak depend on the BD including the temperature dependence, which is different from the R_g behaviour.

The ratio R_g/R_h decreases with decreasing temperature in all samples, reflecting the shrinkage of chains, and details of the change with temperature depend on the BD, as shown in *Figure 9*. The R_g/R_h of CL-1 shifts to lower temperature with the presence of branches. CL-2 has larger R_g/R_h ratios than CL-1. The ratios of RS-8 are lower than those of the others, showing a weak temperature dependence.

At a branch PS composition of 6 wt% (CL-1), with decreasing temperature, the copolymer chain shrinks in the same manner as the PMMA chain with no branches, although the θ-temperature is shifted by the presence of PS branches. This indicates that no particular order structure is formed in CL-1. The differences between the lower BD (CL-1) and the higher BD (CL-2) copolymers, in particular, in R_g and A_2, suggest an essential structural change, that is, a change from a random coil to a unimolecular micelle with intramolecular segregation. In CL-2 and RS-8, the polymer molecule as a whole (in larger scale) has a large excluded volume, while attractive

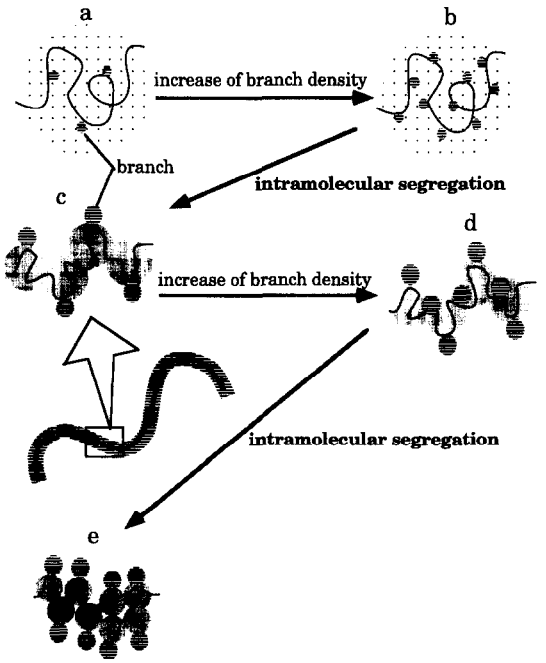

Figure 10 Schematic illustration of intramolecular segregation of graft copolymers induced by increasing branch density. States b and d are unstable and change to more stable states c and e, respectively, which are actually realized. See text for details

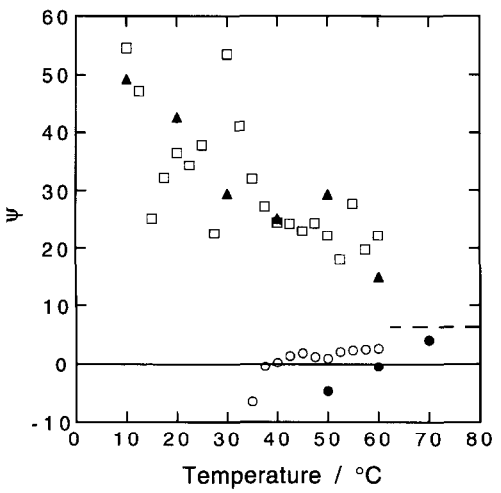

Figure 11 Change of the penetrating function ψ for the graft copolymers and the backbone polymer in i-AA. (○) CL-1; (□) CL-2; (▲) RS-8; (●) CL-b. Broken line indicates the ψ of CL-b in the non-selective good solvent, 1-EN

interactions between backbone-PMMA segments may be localized in short range interaction, and shielded by PS chains with repulsive interaction surrounding the PMMA backbone. The intramolecular segregation is more pronounced in the higher BD sample RS-8 as suggested by the smaller values of R_g and R_g/R_h even at higher temperatures. A tentatively predicted structure will be presented in the following.

Formation of a unimolecular-micelle by intramolecular segregation

As illustrated in *Figure 10*, overlapping of clouds of PMMA and PS would increase with increasing BD if the random coil state was kept (a to b or c to d), and

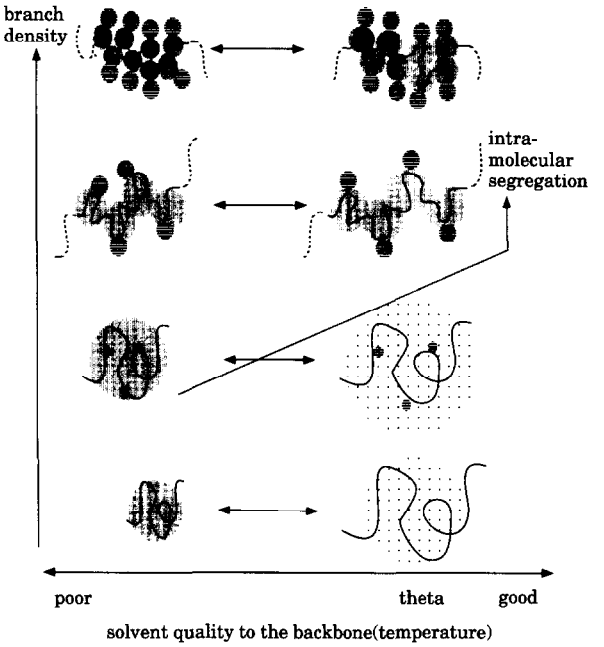

Figure 12 Schematic illustration of estimated structures of PMMA-*g*-PS in i-AA as a function of branch density and solvent quality to the backbone. At lower branch densities, with poorer solvent quality, the graft copolymer chain shrinks in the same manner as the backbone polymer. At higher branch densities, intramolecular segregation occurs to avoid the overlapping of clouds of backbone and branches, which leads to the formation of unimolecular micelles. The intramolecular segregation proceeds more distinctly as the density and the solvent quality becomes poorer

intramolecular segregation may occur to avoid the overlapping (b to c or d to e). As the branch density BD increases further, the separation between backbone and branches may become more distinct by intramolecular segregation (c to e).

The intramolecularly segregated structure must have a characteristic length that is the same as the dimension of a segmental chain between the nearest-neighbour branch points, whatever the structure is. If the unimolecular structure is of a spherical core-corona type, the core size has to be comparable to the segmental-chain dimension. If the structure is rod- or disk-like, then the thickness of the core should be the characteristic length. In the present graft copolymers, the number of PMMA-segmental chains in a molecule is so large (see *Table 2*) that the copolymers may not form a spherical micelle with the core of the segmental-chain, but rather a rod-like micelle to realize intramolecular segregation. The size of the rod-like micelle as a whole depends on another length scale, i.e. the contour length of the whole PMMA-backbone chain. This may lead to shrinkage of the core size (thickness and contour length) with increasing BD and decreasing temperature. This can also explain the weaker temperature dependence of R_g at the higher BD. The intramolecular segregation starts to take place at a BD between those of CL-1 and CL-2, i.e. 6 and 12 wt%, resulting in the formation of a unimolecular micelle. As the attractive interactions between backbone segments increases with decreasing temperature, the intramolecular segregation proceeds more distinctly and the coverage of PMMA backbone chain with PS branches becomes more perfect, which leads to enhancement of the intermolecular repulsion. This is supported experimentally by the

penetrating function for the second virial coefficient, as shown in *Figure 11*. Here, the penetrating function ψ is defined by the equation

$$A_2 = \frac{N_A R_g^3}{M_w^2} \Psi \quad (6)$$

The functions of CL-b and CL-1 have the same magnitude, changing positive to negative with decreasing temperature, whereas those of CL-2 and RS-8 are much larger than those of CL-b and CL-1 and even that of CL-b in good solvent, and greatly increase with decreasing temperature. No difference between CL-2 and RS-8 is found, indicating that the smaller size of the RS-8 chain is responsible for the smaller value of A_2 for RS-8 compared with CL-2.

The above speculations for the chain structure are consistent with the observed differences in R_g/R_h ratio between the different BD copolymers CL-2 and RS-8, i.e. RS-8 has the smaller ratio and weaker temperature dependence because RS-8 may have the more compact rod-like core due to stronger intramolecular segregation.

From the above considerations, the following suggestions are made for the ordered structure of unimolecular micelles. At higher branch densities (CL-2 and RS-8), rod-like unimicelles are formed by intramolecular segregation between the PMMA backbone and PS branches, with the shrunken PMMA backbone making the rod-like core covered with PS chains. With decreasing temperature, the size of the unimolecular micelle decreases, probably with the decrease of the contour length of the micelle core. At the higher branch density, the intramolecular segregation is the stronger and the contour length is the shorter. The rod is not necessarily rigid, but may be flexible in the weakly segregated one and become more rigid as the contour length decreases with stronger segregation.

In *Figure 12*, we summarize these predicted structures of graft copolymers as a function of branch density and solvent quality to the backbone chain.

ACKNOWLEDGEMENTS

The authors thank Professor S. Nakahama and Professor K. Ishizu for assisting with the synthesis of graft copolymers by coupling reaction.

REFERENCES

1 Tuzar, Z. and Kratochivil, P. 'Surface and Colloid Science' (Ed. E. Matijevic), Vol. 15, Plenum Press, New York, p. 1
2 Leibler, L., Oriand, H. and Wheeler, J. C. *J. Chem. Phys.* 1983, **79,** 3550
3 Marques, C., Joanny, J. F. and Leibler, L. *Macromolecules* 1988, **21,** 1051
4 Halperin, A. *Macromolecules* 1987, **20,** 2943
5 Nagarajan, R. and Ganesh, K. *J. Chem. Phys.* 1989, **90,** 5843
6 Noolandi, J. and Hong, K. M. *Macromolecules* 1983, **16,** 1443
7 Munch, M. R. and Gast, A. P. *Macromolecules* 1988, **21,** 1360
8 ten Brinke, G. and Hadziioannou, G. *Macromolecules* 1987, **20,** 1986
9 Honda, C., Sakaki, K. and Nose, T. *Polymer* 1994, **35,** 5309
10 Honda, C., Hasegawa, Y., Hirunuma, R. and Nose, T. *Macromolecules* 1994, **27,** 7660
11 Halperin, A., Tirrel, M. and Lodge, T. P. *Adv. Polym. Sci.* 1992, **100,** 31
12 Balsara, N. P., Tirrell, M. and Lodge, T. P. *Macromolecules* 1991, **24,** 1975
13 Zhou, Z., Chu, B. and Peiffer, D. G. *Macromolecules* 1993, **26,** 1876
14 Chu, B. *Langmuir* 1995, **11,** 414
15 Wu, G. and Chu, B. *Macromolecules* 1994, **27,** 1766
16 Schillen, K., Brown, W. and Konak, C. *Macromolecules* 1993, **26,** 3611
17 Raspand, E., Lairez, D. and Carton, J.-P. *Macromolecules* 1994, **27,** 2956
18 Halperin, A. and Alexander, S. *Macromolecules* 1989, **20,** 2403
19 Selb, J. and Gallot, Y. 'Polymeric Amines and Ammonium Salts' (Ed. E. J. Goethals), Pergamon Press, Oxford, 1980
20 Selb, J. and Gallot, Y. *Makromol. Chem.* 1980, **181,** 809
21 Selb, J. and Gallot, Y. *Makromol. Chem.* 1980, **181,** 2605
22 Selb, J. and Gallot, Y. *Makromol. Chem.* 1981, **182,** 1491
23 Selb, J. and Gallot, Y. *Makromol. Chem.* 1981, **182,** 1513
24 Selb, J. and Gallot, Y. *Makromol. Chem.* 1981, **182,** 1775
25 Price, C. and Woods, D. *Polymer* 1973, **14,** 82
26 Price, C. and Woods, D. *Polymer* 1974, **15,** 389
27 Gallot, T., Franta, E., Remp, P. and Benoit, H. *J. Polym. Sci. Part C* 1964, **4,** 473
28 Dondos, A., Remp, P. and Benoit, H. *J. Chim. Phys.* 1965, **62,** 821
29 Dondos, A., Remp, P. and Benoit, H. *J. Polym. Sci., Polym. Lett. Ed.* 1966, **4,** 293
30 Bresler, S. E., Pyrkov, L. M., Frenkel, S. Ya., Laius, L. A. and Klenin, S. II. *Vysokomol. Soedin.* 1962, **4,** 250
31 Kotaka, T., Tanaka, T. and Inagaki, H. *Polym. J.* 1972, **3,** 327
32 Tanaka, T. and Kotaka, T. and Inagaki, H. *Polym. J.* 1972, **3,** 338
33 Spevacek, J. *Makromol. Chem., Rapid. Commun.* 1982, **3,** 697
34 Plestil, J. and Baldrian, J. *Makromol. Chem.* 1975, **176,** 1009
35 Halperin, A. *Macromolecules* 1991, **24,** 1418
36 de Gennes, P. G. *Israel. J. Chem.* 1995, **35,** 33
37 Joanny, J. F. and Leibler, L. *J. Phys. Fr.* 1990, **51,** 545
38 Khokhlov, A. R. *J. Phys. A, Math. Gen.* 1980, **13,** 979
39 Kikuchi, A. and Nose, T. *Polymer* 1995, **36,** 2781
40 Benoit, H. and Froelich, D. 'Light Scattering from Polymer Solutions' (Ed. M. B. Huglin), Chap. 11 Academic Press, New York, 1972
41 Varma, B., Fujita, Y., Takahashi, M. and Nose, T. *J. Polym. Sci., Polym. Phys. Ed.* 1984, **22,** 1181
42 Brunel, R. F. and Bibber, K. V. 'International Critical Tables' (Eds C. J. West, N. E. Dorsy, F. R. B. Chowsky and A. K. Klemenc), Vol. 3, McGraw-Hill, New York, p. 27
43 Dixon, A. L. and West, C. J. 'International Critical Tables' (Eds C. J. West, N. E. Dorsy, F. R. B. Chowsky and A. K. Klemenc), Vol. 7, McGraw-Hill, New York, p. 34
44 Kirste, R. and Schulz, G. *V. Z. Phys. Chem. Neue Folge* 1961, **27,** 301
45 Koppel, D. E. *J. Chem. Phys.* 1974, **57,** 4814